Asian Journal of Chemistry; Vol. 27, No. 10 (2015), 3907-3912

ASIAN JOURNAL OF CHEMISTRY

http://dx.doi.org/10.14233/ajchem.2015.19068

Computational and Spectral Studies of Nimesulide Impurity D: 4-Nitro-2-phenoxy Aniline

S. ANIL KUMAR and B.L. BHASKAR*

Department of Chemistry, Amrita Vishwa Vidyapeetham, Amrita School of Engineering, Bangalore-560 035, India

*Corresponding author: Fax: +91 80 28440092; Tel: +91 80 25183700 E-mail: basee77@gmail.com

Received: 30 January 2015; *Accepted*: 4 March 2015; *Published online*: 22 June 2015; AJC-17371

The present work describes the structural and spectral characterization studies of 4-nitro-2-phenoxy aniline, which is an intermediate product during the synthesis of nimesulide, by both computational and experimental methods. Characteristic IR absorption frequencies were computed by Gaussian 03 using density function methods at B3LYP/6-311G, B3LYP/6-31G basis sets and Hartree Fock methods at HF 3-21G basis set. Theoretical XRD data was generated by Gaussian 03 at different basis sets and data consolidated to show concordance with experimental data available in the literature and also corroborate the presence of intra-molecular hydrogen bonding. The HOMO and LUMO energy gap value has been computed to be around 4 eV indicating relatively high reactivity of the compound. In general, computational and experimental data showed satisfactory concurrence with each other.

Keywords: 4-Nitro-2-phenoxy aniline, Computational, DFT, Gaussian 03.

INTRODUCTION

4-Nitro-2-phenoxy aniline (**I**) is an intermediate for the synthesis of nimesulide which is the first COX-2 selective non steroidal anti inflammatory drug (NSAID)[1,2]. 4-Nitro-2-phenoxy aniline is a derivative of biphenyl ether having a twin aromatic ring structure[3]. Biphenyl ether derivatives have many biological and organic chemistry applications. Certain Schiff bases containing 4-nitro-2-phenoxy aniline has been synthesized and studied by Shreenivas *et al.*[4]. Interestingly in their attempt to study Schiff bases they have come across a possible idea of using 4-nitro-2-phenoxy aniline as a possible alternate to losartan. It was reported that 4-nitro-2-phenoxy aniline was able to reduce angiotension-II induced hypertension and also phenyl epinephrine induced vasoconstriction comparable with losartan. The same authors were hopeful that this molecule may be taken as a lead molecule for angiotensin induced hypertension and it may not be necessary to go for the synthesis of a big molecule.

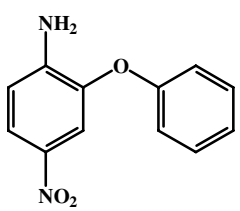

Structure of 4-nitro 2-phenoxy aniline (**I**)

In addition to the pharmacological properties, the impurities present also play an important role in defining the efficiency and safety of a drug. Since these impurities are produced during synthetic process, any slight changes in the processes cause changes in impurity profile. At times, reaction intermediates also carry forward and causes concerns about safety. Process changes are common as a drug molecule is carried through development and the process is scaled up and optimized. Also, when generic versions of a currently marketed drug are produced, the synthetic processes are likely to be different from the one used by the original manufacturer[5].

HPLC separation of nimesulide and its impurities including 4-nitro-2-phenoxy aniline using a narrow bore monolithic column has been discussed by Zacharis and Tzanavaras[6]. Simultaneous determination of nimesulide and 4-nitro-2-phenoxy aniline in pharmaceutical formulations by reversed phase high performance liquid chromatography has been reported by Tubic *et al.*[7].

The crystal structure of 4-nitro-2-phenoxy aniline was studied by Manjunath *et al.*[2] and according to them the oxygen atom bridging the two aromatic rings is in *syn*-periplanar ($^{+}$sp) conformation. The dihedral angle between the aromatic rings is reported to be 71.40(12)°. They have also reported that in the crystal, the molecules are linked by intermolecular N–H–O hydrogen bonds[3]. To the best of our knowledge no comprehensive computational calculations were reported for the molecule 4-nitro-2-phenoxy aniline.

In the present work, 4-nitro-2-phenoxy aniline was characterized using FTIR studies. The resultant experimental data have been compared with computational methods using DFT and HF approximations. Similarly the XRD data derived from computational methods have been compared with the reported XRD data in the literature method[3]. In general computational and experimental data showed satisfactory concurrence with each other.

EXPERIMENTAL

The FTIR spectra of the compound was recorded with a Perkin Elmer instrument in the range 4000-400 cm^{-1} using KBr pellet method (1:100). Single crystal X-ray diffraction studies of 4-nitro-2-phenoxy aniline were performed and the crystal structure was predicted by Manjunath *et al.*[3]. The same XRD data has been utilized here for comparison.

Computational details

The molecular mechanics and *ab initio* quantum chemical calculations of 4-nitro-2-phenoxy aniline was studied using Gaussian 03 tool packages at suitable basis sets[8]. The optimized molecular structure of the title compound in the ground state was figured out by Gaussian 03W program package using *ab initio* Density Functional Theory (DFT) approximations using 6-311++G(d,p) and 6-31++G(d,p) basis sets (Fig. 1). The title molecule contains 27 atoms and 75 possible IR vibrations were reported by DFT analysis assuming C1 symmetry. The optimized molecular structure with scheme of atom numbering of 4-nitro-2-phenoxy aniline is shown in Fig. 2.

DFT method including local or non-local functional, yields molecular force fields and vibrational wave numbers in good agreement with experimental results[9]. In DFT methods Becke's three parameter exact exchange-functional (B3)[10-12] combined with gradient-corrected correlational functional of Lee, Yang and Parr (LYP)[13] by implementing the split-valence polarized 6-31G(d,p) and 6-311G(d,p) basis sets[14] have been

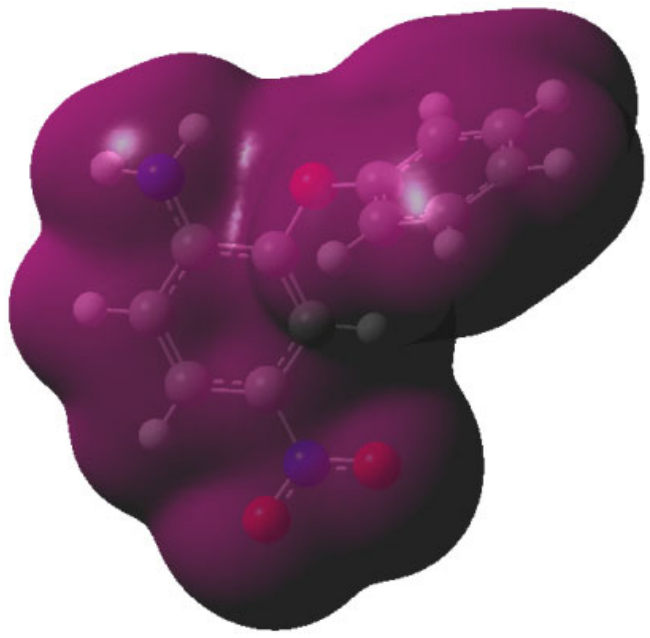

Fig. 1. 3D structure of 4-nitro 2-phenoxy aniline as visualized by Gaussian 03 using DFT method at B3LYP/6-311G basis set

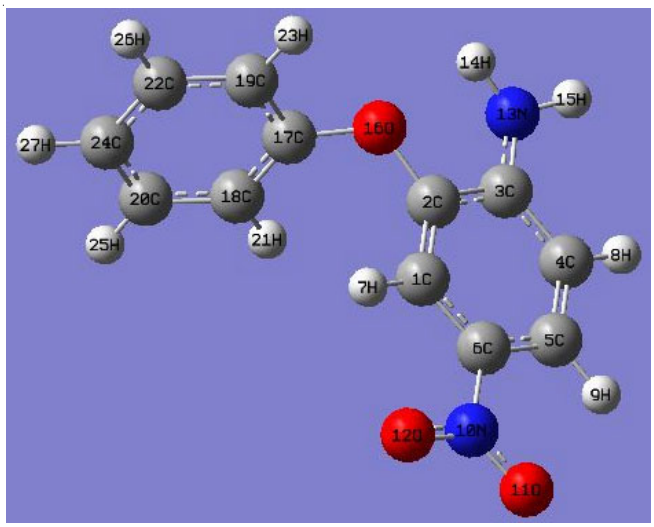

Fig. 2. Optimized molecular structure of 4-nitro 2-phenoxy aniline

utilized for the computation of properties. The calculations were also performed using Hartree Fock (HF) methods at 3-21G(d,p) basis set. Computed IR frequencies from HF methods are relatively higher due to the possible over estimation of vibrational modes as the anharmonicity experienced in the real system is neglected. Values obtained from DFT methods as relatively smaller and closer to experimental FTIR frequencies probably because of the inclusion of electron correlation[15]. In general, computed IR frequencies after applying suitable scaling factors, show satisfactory agreement with each other and also with FTIR data (Tables 1-3 and Figs. 3-5).

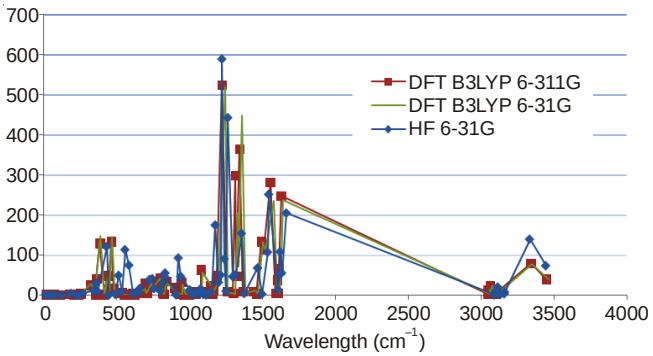

Fig. 3. Computed FTIR spectra using different basis sets

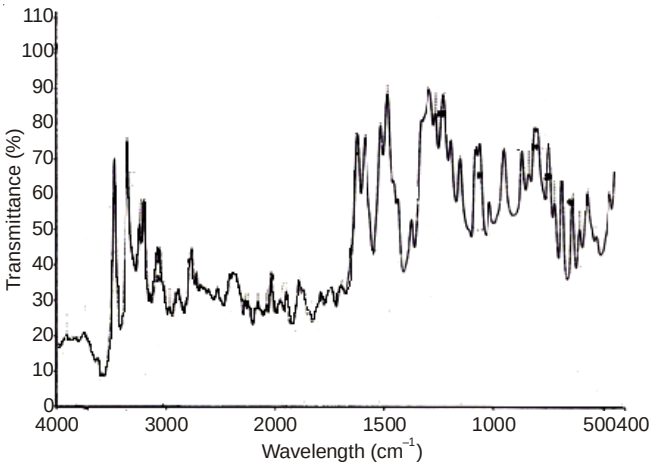

Fig. 4. Experimental FTIR spectrum of 4-nitro 2-phenoxy aniline

TABLE-1
COMPARISON OF COMPUTATIONAL AND EXPERIMENTAL VIBRATIONAL FREQUENCIES OF 4-NITRO-2-PHENOXY ANILINE

S. No.	DFT B3LYP 6-311G			DFT B3LYP 6-31G			HF 3-21G			Expt. IR	Assignment
	Frequency		Int.	Frequency		Int.	Frequency		Int.		
	Unscaled	Scaled		Unscaled	Scaled		Unscaled	Scaled			
1	3704.33	3445.03	39.40	3725.00	3464.25	38.73	3913.85	3444.19	73.34	3474	Ar NH_2 (asym str.)
2	3591.38	3339.98	78.20	3602.50	3350.33	77.15	3787.80	3333.26	139.57	3350	Ar NH_2 (sym str.)
3	3227.00	3097.92	5.30	3250.80	3120.77	4.60	3437.00	3162.04	7.60		νC-H
4	3227.00	3097.92	2.10	3248.60	3118.66	1.60	3434.00	3159.28	3.30		νC-H
5	3199.00	3071.04	2.50	3218.90	3090.14	0.80	3403.00	3130.76	1.07		νC-H
6	3196.14	3068.29	8.50	3216.05	3087.41	9.90	3399.00	3127.08	3.40		νC-H
7	3189.10	3061.54	21.68	3207.86	3079.55	24.13	3385.78	3114.92	20.22	3081	νC-H
8	3177.60	3050.50	8.37	3195.00	3067.20	9.80	3380.40	3109.97	8.90		νC-H
9	3172.77	3045.86	12.68	3191.50	3063.84	12.90	3370.50	3100.86	9.20	3052	νC-H
10	3168.90	3042.14	1.35	3186.00	3058.56	1.40	3360.00	3091.20	0.35		νC-H
11	1660.24	1627.04	246.90	1671.43	1638.00	236.97	1808.30	1663.64	204.83	1626	N-H bending
12	1646.00	1613.08	64.50	1660.70	1627.49	90.87	1774.10	1632.17	55.37		νCC
13	1636.00	1603.28	4.03	1652.00	1618.96	4.31	1762.00	1621.04	108.30		νCC
14	1633.24	1600.58	36.50	1646.85	1613.91	42.53	1758.89	1618.18	50.69		νCC
15	1624.00	1591.52	4.09	1631.30	1598.67	3.70	1746.69	1606.95	13.56	1588	νC-NO_2
16	1584.00	1552.32	280.83	1606.44	1574.31	234.50	1676.43	1542.32	251.40		νCC
17	1537.50	1506.75	113.70	1550.00	1519.00	111.20	1668.95	1535.43	107.19	1515	νCC
18	1521.25	1490.83	132.80	1533.62	1502.95	131.68	1627.00	1496.84	2.70	1484	νCC
19	1488.00	1458.24	2.40	1498.90	1468.92	2.15	1593.56	1466.08	67.71		νCC
20	1465.00	1435.70	7.60	1476.16	1446.64	10.94	1494.00	1374.48	4.10		νCC
21	1392.00	1364.16	7.70	1406.60	1378.47	4.30	1473.20	1355.34	154.07	1379	νC-NO_2
22	1367.50	1340.15	363.40	1387.36	1359.61	447.26	1428.51	1314.23	50.36		νCC
23	1348.45	1321.48	45.90	1362.23	1334.99	70.10	1408.42	1295.75	46.24		νCC
24	1341.28	1314.45	296.97	1354.89	1327.79	205.20	1371.77	1262.03	442.80	1295	νC-NH_2
25	1324.90	1298.40	4.36	1336.57	1309.84	2.10	1359.00	1250.28	9.90		νCC
26	1282.72	1257.07	8.25	1285.00	1259.30	6.80	1346.14	1238.45	90.59		νCC
27	1246.43	1221.50	522.67	1265.46	1240.15	519.10	1327.50	1221.30	589.25	1230	νC-O-C
28	1211.59	1187.36	47.10	1221.60	1197.17	34.32	1318.04	1212.60	49.95	1196	βCH, νC-O-C
29	1184.28	1160.59	12.91	1190.70	1166.89	10.10	1302.40	1198.21	31.73		βCH
30	1179.00	1155.42	3.08	1185.00	1161.30	1.63	1277.47	1175.27	174.84		βCH
31	1167.52	1144.17	23.50	1171.94	1148.50	21.73	1247.00	1147.24	7.50		βCH
32	1098.99	1077.01	62.29	1107.17	1085.03	56.25	1210.00	1113.20	0.29	1085	C-O-C
33	1097.94	1075.98	8.21	1104.20	1082.12	6.70	1190.30	1095.08	1.56	1068	ρNH_2
34	1064.00	1042.72	3.05	1067.60	1046.25	2.30	1189.70	1094.52	6.80		βCH
35	1043.90	1023.02	6.80	1049.60	1028.61	5.02	1187.00	1092.04	9.70		βCH
36	1017.00	996.66	0.67	1017.50	997.15	1.47	1166.80	1073.46	15.32		βCH
37	996.60	976.67	0.05	992.50	972.65	0.23	1161.40	1068.49	4.60		δNH_2
38	976.30	956.77	0.36	970.14	950.74	26.74	1133.00	1042.36	2.40		βCH
39	965.74	946.43	31.59	968.50	949.13	0.34	1130.30	1039.88	4.80		γCH
40	962.00	942.76	1.98	960.80	941.58	0.58	1106.80	1018.26	2.50		γCH
41	921.40	902.97	7.50	919.00	900.62	8.20	1087.53	1000.53	13.15		γCH
42	913.90	895.62	17.80	911.90	893.66	11.64	1020.15	938.54	46.67		γCH
43	858.43	841.26	33.40	856.48	839.35	29.56	1002.53	922.33	92.70	843	δNO_2
44	838.80	822.02	1.48	840.90	824.08	1.10	986.00	907.12	0.45		γCH
45	830.80	814.18	3.36	832.00	815.36	4.50	903.27	831.01	55.09		γCH
46	825.63	809.12	27.37	828.95	812.37	17.12	897.95	826.11	47.36		γCH
47	813.30	797.03	40.65	808.79	792.61	40.47	887.28	816.30	30.38		γCH
48	766.85	751.51	24.27	766.99	751.65	21.90	868.00	798.56	10.30	752	ωN-H_2
49	740.64	725.83	25.74	750.35	735.34	28.23	820.99	755.31	16.33	724	βCCC
50	722.70	708.25	4.98	714.70	700.41	5.08	808.35	743.68	41.05		βCCC
51	706.08	691.96	27.89	702.70	688.65	14.00	787.19	724.21	38.92	691	βCCC
52	659.00	645.82	4.02	659.20	646.02	5.30	714.08	656.95	16.47	645	ωNO_2
53	633.20	620.54	0.42	632.00	619.36	0.50	708.00	651.36	6.90		βCCC
54	618.00	605.64	2.70	617.80	605.44	2.06	686.50	631.58	6.00		βCCO
55	596.60	584.67	0.89	597.00	585.06	0.33	663.00	609.96	3.80	577	βCCO
56	561.00	549.78	0.68	562.00	550.76	0.54	633.96	583.24	74.68		βCCC
57	544.00	533.12	5.29	544.30	533.41	3.90	603.78	555.48	113.35		ρNO_2

58	487.55	477.80	15.88	491.00	481.18	8.80	579.00	532.68	9.07		βCCC, βC-NH_2
59	471.17	461.75	132.95	473.89	464.41	144.25	556.38	511.87	49.29		βCCO
60	452.25	443.21	13.32	455.89	446.77	10.00	531.80	489.26	1.80		βCCC
61	443.70	434.83	47.77	444.55	435.66	47.17	482.60	443.99	0.06		γC-NO_2
62	423.00	414.54	0.47	423.00	414.54	0.38	481.00	442.52	0.23	475	βCCC, ωNH_2
63	392.30	384.45	128.47	393.37	385.50	146.90	466.02	428.74	120.77		βCCC
64	367.70	360.35	40.20	365.33	358.02	33.90	402.60	370.39	8.40		γCCC
65	358.70	351.53	0.93	358.19	351.03	10.16	389.61	358.44	29.67		γCCC
66	324.75	318.26	24.27	327.97	321.41	27.76	371.38	341.67	11.10		βCCO
67	257.00	251.86	2.90	259.60	254.41	3.50	288.00	264.96	4.20		γCCC
68	242.00	237.16	0.35	242.60	237.75	0.16	259.90	239.11	0.25		βCCO
69	205.70	201.59	0.69	210.00	205.80	0.64	241.70	222.36	0.22		γCCC
70	181.00	177.38	1.22	183.00	179.34	1.20	201.00	184.92	4.00		γCCC
71	113.00	110.74	0.16	115.90	113.58	0.24	136.00	125.12	0.19		γCCC
72	70.00	68.60	1.50	75.00	73.50	1.29	85.00	78.20	0.60		τNO_2
73	54.70	53.61	0.52	57.00	55.86	0.68	59.60	54.83	0.58		γCCC
74	33.50	32.83	0.55	31.00	30.38	0.59	33.00	30.36	0.57		γCCC
75	14.70	14.41	0.70	16.00	15.68	0.60	12.70	11.68	0.90		γCCC

ν-Stretching; β-In-plane bending; δ-Deformation; ρ-Rocking; γ-Out-of-plane bending; ω-Wagging; τ-Torsion

TABLE-2
OPTIMIZED COMPUTATIONAL BOND LENGTHS AT HF 3-21G, B3LYP 6-311G AND B3LYP 6-31G FOR 4-NITRO-2-PHENOXY ANILINE

S. No.	Bond length	XRD data	HF/3-21G	B3LYP/6-311G(d,p)	B3LYP/6-31G(d,p)
1	C5-C6	1.38	1.38	1.39	1.39
2	C1-C6	1.39	1.38	1.40	1.40
3	C6-N10	1.44	1.43	1.46	1.46
4	C4-C5	1.37	1.37	1.39	1.39
5	C5-H9	0.93	1.07	1.08	1.08
6	C3-C4	1.39	1.40	1.40	1.41
7	C4-H8	0.93	1.07	1.08	1.09
8	C3-N13	1.36	1.35	1.37	1.37
9	C3-C2	1.41	1.40	1.42	1.42
10	C1-C2	1.37	1.36	1.38	1.38
11	C2-O16	1.38	1.39	1.38	1.38
12	C1-H7	0.93	1.07	1.08	1.08
13	N10-O12	1.23	1.25	1.23	1.23
14	N10-O11	1.23	1.25	1.23	1.23
15	N13-H14	0.86	1.00	1.01	1.01
16	N13-H15	0.86	0.99	1.01	1.01
17	O16-C17	1.39	1.40	1.39	1.39
18	C17-C19	1.35	1.38	1.39	1.39
19	C17-C18	1.37	1.38	1.39	1.40
20	C19-C22	1.36	1.38	1.39	1.40
21	C19-H23	0.93	1.07	1.08	1.08
22	C22-C24	1.34	1.39	1.39	1.40
23	C22-H26	0.93	1.07	1.08	1.09
24	C24-C20	1.37	1.38	1.39	1.40
25	C24-H27	0.93	1.07	1.08	1.09
26	C20-C18	1.40	1.38	1.39	1.39
27	C20-H25	0.93	1.07	1.08	1.08
28	C18-H21	0.93	1.07	1.08	1.08

HOMO-LUMO Energy gap: Energies of frontier molecular orbitals were calculated at B3LYP/6-311G and B3LYP/6-31G basis sets. It is useful to study energies of the highest occupied molecular orbital (HOMO) and the lowest unoccupied molecular orbital (LUMO) as these are the ones partaking in reactions. The energy of HOMO orbital throws light into the ability of electron donation while LUMO energy provides information about ability of electron receiving and the gap between HOMO and LUMO symbolizes the chemical stability

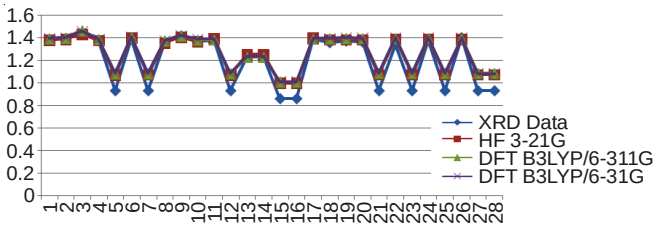

Fig. 5(a). Comparison of bond lengths between experimental and computational approaches

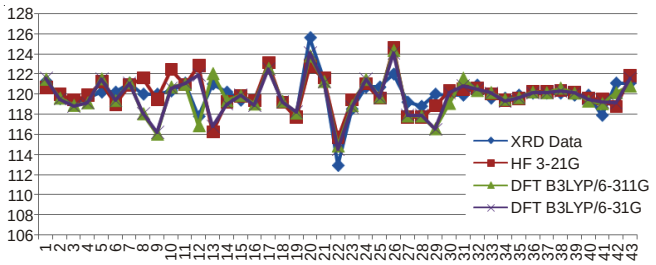

Fig. 5(b). Comparison of bond angles between experimental and computational approaches

of the molecule[16]. The HOMO and LUMO energy gap value is found to be around 4 eV indicating relatively high reactivity of the compound (Table-4 and Fig. 6).

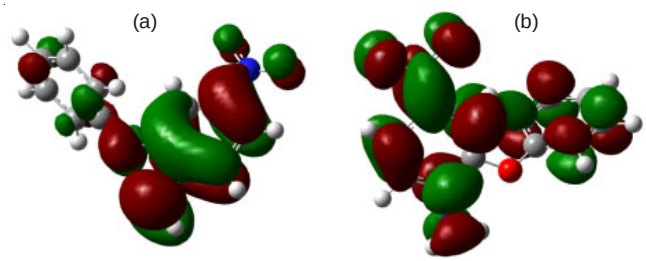

Fig. 6. (a) HOMO and (b) LUMO

RESULTS AND DISCUSSION

Geometrical structure: The optimized molecular structure of 4-nitro-2-phenoxy aniline deduced at B3LYP 6-311++G (d,p) basis set using density function theory is shown in Fig. 2

TABLE-3
OPTIMIZED COMPUTATIONAL BOND ANGLES AT HF 3-21G, B3LYP 6-311G AND B3LYP 6-31G FOR 4-NITRO-2-PHENOXY ANILINE

S. No.	Bond angle	XRD Data	HF/3-21G	B3LYP/6-311G(d,p)	B3LYP/6-31G(d,p)
1	C5-C6-C1	121.29	120.63	121.48	121.60
2	C5-C6-N10	119.55	119.95	119.62	119.50
3	C1-C6-N10	119.14	119.42	118.90	118.80
4	C4-C5-C6	119.54	119.85	119.14	119.10
5	C4-C5-H9	120.20	121.20	121.51	121.50
6	C6-C5-H9	120.20	118.96	119.35	119.40
7	C5-C4-C3	121.10	120.89	121.11	121.10
8	C3-N13-H14	120.00	121.57	118.05	118.10
9	H14-N13-H15	120.00	119.46	116.03	116.20
10	C2-O16-C17	120.32	122.44	120.70	120.60
11	C19-C17-C18	121.10	120.91	120.99	121.10
12	C19-C17-O16	117.80	122.80	116.87	121.90
13	C18-C17-O16	121.00	116.20	122.04	116.80
14	C17-C19-C22	120.20	119.20	119.34	119.00
15	C5-C4-H8	119.40	119.80	119.85	119.90
16	C3-C4-H8	119.40	119.30	119.03	118.90
17	N13-C3-C4	122.70	123.10	122.56	122.50
18	N13-C3-C2	119.24	119.15	119.28	119.20
19	C4-C3-C2	118.06	117.67	118.13	118.20
20	C1-C2-O16	125.60	122.73	123.78	124.10
21	C1-C2-C3	121.45	121.57	121.26	121.20
22	O16-C2-C3	112.93	115.65	114.84	114.50
23	C2-C1-C6	118.53	119.39	118.86	118.70
24	C2-C1-H7	120.70	121.00	121.45	121.50
25	C6-C1-H7	120.70	119.56	119.69	119.60
26	O12-N10-O11	121.99	124.58	124.35	124.10
27	O12-N10-C6	119.21	117.70	117.83	117.90
28	O11-N10-C6	118.80	117.70	117.82	117.90
29	C3-N13-H14	120.00	118.80	116.56	116.50
30	C17-C19-H23	119.90	120.30	119.08	120.10
31	C22-C19-H23	119.90	120.45	121.58	120.80
32	C24-C22-C19	120.90	120.53	120.36	120.50
33	C24-C22-H26	119.60	120.00	120.15	120.10
34	C19-C22-H26	119.60	119.36	119.48	119.30
35	C22-C24-C20	119.90	119.54	119.64	119.60
36	C22-C24-H27	120.10	120.22	120.21	120.10
37	C20-C24-H27	120.10	120.22	120.14	120.10
38	C24-C20-C18	120.10	120.32	120.59	120.30
39	C24-C20-H25	119.90	120.10	120.10	120.10
40	C18-C20-H25	119.90	119.57	119.31	119.50
41	C17-C18-C20	117.90	119.48	119.06	119.20
42	C17-C18-H21	121.10	118.74	120.14	119.10
43	C20-C18-H21	121.10	121.77	120.79	121.60

with the scheme of atom numbering. The computational bond lengths and bond angles were compared with each other and also with the experimental data and were shown in Tables 2 and 3. The calculated data shows slight deviations from the experimental values for the reason that computations are possibly calculated assuming single crystal in gas phase sans any inter-molecular interactions. In addition, the layered stacking interactions of the molecule were also ignored in absolute vacuum. The XRD data reveals the bond angle at C1-C2-O16 to be 125.6 indicating possible expansion due to intra-molecular hydrogen bonding. Similarly a contraction of bond angle (112.93) at C3-C2-O16 endorses the presence of intra-molecular hydrogen bonding. DFT studies also corroborate the same with relatively higher bond angle at C1-C2-O16 {122.7 at HF/3-21G, 123.8 at B3LYP/6-311G and 124.1 at B3LYP/6-31G} and shorter one at C3-C2-O16 {115.65 at HF/3-21G, 114.84 at B3LYP/6-311G and 114.50 at B3LYP/6-31G}.

Determination of scaling factor: Computational vibrational frequencies upon appropriate scaling show good agreement with experimental data. For Ar-NH_2 asymmetric stretching at 3704 cm^{-1} and Ar-NH_2 symmetric stretching at 3591 cm^{-1} a scaling factor of 0.93 has been used. For C-H stretching vibrations above 3000 cm^{-1} a scaling factor of 0.96 has been used. For all other vibrations a scaling factor of 0.98 has been used.

Vibrational frequencies and assignments

NH_2- vibrations: The expected band of absorption for stretching vibration of aromatic amine is between 3500-3300 cm^{-1}. Therefore the vibrations at 3474 cm^{-1} and 3350 cm^{-1} observed in the experimental spectrum are attributed to asymmetric stretching and symmetric stretching of aromatic amines respectively. The computational analysis also correlate this with the presence of strong bands at 3445 and 3340 cm^{-1} (DFT B3LYP 6-311G), 3464 and 3350 cm^{-1} (DFT B3LYP6-31G) and 3444 and 3333 cm^{-1} (HF 3-21G). The in-plane bending vibration mode of NH_2- (1650-1580 cm^{-1}) is seen at 1626 cm^{-1} in the experimental spectra and at 1627 cm^{-1} in the computa-tional data (high intense). The C-NH_2 stretching mode is identified as the broad peak at 1295 cm^{-1} in IR spectra and the same has been visualized in computed data as the high intense absorption at 1298 cm^{-1}. The in-plane rocking mode of amino group usually found at 1150-900 cm^{-1} has been observed at 1068 and 1076 cm^{-1} in experimental and computational analysis respectively.

The out of plane deformation band of NH_2 is computed at 977 cm^{-1} (weak) but the same is not visible in the experimental spectrum. The bands seen at 751 and 477 cm^{-1} in the computation are attributed to wagging and twisting modes of amino group. Though wagging is visible in the experimental graph as a peak at 752 cm^{-1}, twisting mode is not clearly seen.

NO_2 vibrations: The presence of NO_2 is confirmed by the presence of intense bands at 1588 and 1379 cm^{-1} representing asymmetric and symmetric C-NO_2 stretching vibrations respectively. These vibrational assignments are endorsed by *ab initio* computation by the presence of very strong bands at 1591 and 1379 cm^{-1}. The IR spectrum also reveals bands at 843 and 645 cm^{-1} which are attributed to deformation and wagging by NO_2 respectively. The computed data also corroborate this with presence of bands at 841 and 645 cm^{-1} respectively. Other vibrational modes due to rocking, out of

TABLE-4
HOMO-LUMO ENERGIES

Basis set	HOMO	LUMO	HOMO-1	LUMO+1	HOMO-LUMO energy gap
DFT B3LYP 6-311G	-0.226	-0.079	-0.251	-0.031	4.00 eV
DFT B3LYP 6-31G	-0.218	-0.072	-0.242	-0.020	3.97 eV

plane bending and torsion are noted in the computation at wavelengths 533, 434 and 69 cm^{-1} respectively.

C-O-C vibrations: C-O stretching vibrations of aromatic ether generally appear as medium or strong bands at 1270-1230 cm^{-1} and the experimental spectrum clearly shows 3 medium peaks at 1230, 1196 and 1085 cm^{-1}. The vibration modes above 1200 cm^{-1} result from C-O asymmetric stretching and those below 1200 cm^{-1} are possibly due to symmetric stretching[17]. The corresponding modes are visualized at (1221, 1187, 1077 cm^{-1}), (1240, 1197, 1085 cm^{-1}) and (1221, 1212, 1113 cm^{-1}) for DFT/B3LYP/6-311G, DFT/B3LYP/6-31G and HF/3-21G approximations respectively.

C-H vibrations: Generally C-H stretching vibrations have been observed between 3100-3000 cm^{-1} range. For 4-nitro-2-phenoxy aniline 8 C-H stretching vibrations have been computed at 3097, 3097, 3071, 3068, 3061, 3050, 3046 and 3042 cm^{-1} using DFT/B3LYP/6-311G basis set. These correspond to 8 aromatic C-H bonds and are comparable with experimental values at 3081 and 3052 cm^{-1}. The symmetric C-H in-plane bending vibrations are observed at 1300-850 cm^{-1} as weak bands[18] and the C-H out of plane bending vibrations of medium intensities are observed[18] in the region 950-600 cm^{-1}. The computed modes at 1187, 1160, 1155, 1144, 1043, 1023, 993 and 956 cm^{-1} and those at 1197, 1167, 1161, 1148, 1046, 1028, 1017 and 950 cm^{-1} correspond to 8 C-H in-plane bending vibrations for DFT/B3LYP/6-311G and DFT/B3LYP/6-31G respectively. The corresponding C-H in-plane bending vibrations for HF/3-21G are computed at 1212, 1198, 1175, 1147, 1094, 1092, 1079 and 1042 cm^{-1}. Similarly out-of-plane C-H bending modes are visualized at 8 modes {946, 942, 903, 895, 822, 814, 809, 797 and 949, 941, 901, 894, 824, 815, 812, 792 and 1039, 1018, 1000, 938, 907, 831, 826, 816 cm^{-1} for DFT/B3LYP/6-311G, DFT/B3LYP/6-31G and HF/3-21G approximations respectively}.

Conclusions

4-Nitro-2-phenoxy aniline has C1 symmetry and possesses 75 possible vibrations. The experimental data and computed data upon scaling show good agreement on comparison and slight differences are attributed to the fact that computational calculations are done considering single molecule in gaseous state sans intermolecular interactions. Density function theory based computations emerge to be more consistent with the experimental values as compared to Hartree Fock approximations, the possible reason being over estimation due to disregard of system anharmonicity.

The XRD data reveals the bond angle at C1-C2-O16 to be 125.6 indicating possible expansion due to intra-molecular hydrogen bonding. Similarly a contraction of bond angle (112.93) at C3-C2-O16 endorses the presence of intra-molecular hydrogen bonding. DFT studies also corroborate the same with relatively higher bond angle at C1-C2-O16 and shorter one at C3-C2-O16. The HOMO and LUMO energy gap value has been computed to be around 4 eV indicating relatively high reactivity of the compound.

REFERENCES

1. G.G.L. Moore and J.K. Harrington, US Patent No. 3840597 (1974).
2. A. Prasad, M.L. Sharma, S. Kanwar, R. Rathee and S.D. Sharma, *J. Sci. Ind. Res.*, **64**, 756 (2005).
3. H.R. Manjunath, M.T. Shreenivasa, M. Mahendra, T.M. Mohan Kumar, B.E. Kumaraswamy and M.A. Sridhar, *Acta Crystallogr.*, **66E**, 1255 (2010).
4. M.T. Shreenivasa, B.P. Chetan and A.R. Bhat, *J. Pharm. Sci. Technol.*, **1**, 88 (2009).
5 E.C. Nicolas and T.H. Scholz, *J. Pharm. Biomed. Anal.*, **16**, 813 (1998).
6. C.K. Zacharis and P.D. Tzanavaras, *Chromatographia*, **73**, 347 (2011).
7. B. Tubic, B. Ivkovic, M. Zecevic and S. Vladimirov, *Acta Chim. Slov.*, **54**, 583 (2007).
8. M. Frisch, G.W. Trucks, H.B. Schlegel, G.E. Scuseria, M.A. Robb, J.R. Cheeseman, G. Scalmani, V. Barone, B. Mennucci, G.A. Petersson, H. Nakatsuji, M. Caricato, X. Li, H.P. Hratchian, A.F. Izmaylov, J. Bloino, G. Zheng, J.L. Sonnenberg, M. Hada, M. Ehara, K. Toyota, R. Fukuda, J. Hasegawa, M. Ishida, T. Nakajima, Y. Honda, O. Kitao, H. Nakai, T. Vreven, J.R.Montgomery Jr, J.E. Peralta, F. Ogliaro, M. Bearpark, J.J. Heyd, E. Brothers, K.N. Kudin, V.N. Staroverov, R. Kobayashi, J. Normand, K. Raghavachari, A. Rendell, J.C. Burant, S.S. Iyengar, J. Tomasi, M. Cossi, N. Rega, J.M. Millam, M. Klene, J.E Knox, J.B. Cross, V. Bakken, C. Adamo, J. Jaramillo, R. Gomperts, R.E. Stratmann, O. Yazyev, A.J. Austin, R. Cammi, C. Pomelli, J.W. Ochterski, R.L. Martin, K. Morokuma, V.G. Zakrzewski, G.A. Voth, P. Salvador, J.J. Dannenberg, S. Dapprich, A.D. Daniels, O. Farkas, J.B. Foresman, J.V. Ortiz, J. Cioslowski and D.J. Fox, Gaussian Inc., Wallingford, CT (2009).
9. M.M. El-Nahass, M.A. Kamel, A.A. El-Barbary, M.A.M. El-Mansy and M. Ibrahim, *Spectrochim. Acta A*, **111**, 37 (2013).
10. A.D. Becke, *Phys. Rev. A*, **38**, 3098 (1988).
11. A.D. Becke, *J. Chem. Phys.*, **98**, 5648 (1993).
12. B.G. Johnson and M.J. Frisch, *Chem. Phys. Lett.*, **216**, 133 (1993).
13. C. Lee, W. Yang and R.G. Parr, *Phys. Rev. B*, **37**, 785 (1988).
14. V. Arjunan, P.S. Balamourougane, C.V. Mythili and S. Mohan, *J. Mol. Struct.*, **1003**, 92 (2011).
15. T. Prabhu, S. Periandy and S. Mohan, *Spectrochim. Acta A*, **78**, 566 (2011).
16. I. Fleming, Frontier Orbitals and Organic Chemical Reactions, Wiley, London, 1976.
17. S. Qiu, L. Liu, X. Jin, A. Zhang, K. Wu and L. Wang, *Spectrochim. Acta A*, **77**, 572 (2010).
18. V. Arjunan, P. Ravindran, T. Rani and S. Mohan, *J. Mol. Struct.*, **988**, 91 (2011).